Journal of Experimental and Clinical Application of Chinese Medicine

ORIGINAL RESEARCH

Open Access

Screening of α-Glucosidase Inhibitors in Extracts of *Polygonum bistorta* Based on Spectrum-Effect Relationship

Qi Huang [1,#], Weiqi Yang [1,#], Xiaofei Li [1,2], Liqiao Xie [1,3], Dan Tang [2,*], Zhengming Qian [1,*]

1. Dongguan HEC Cordyceps R&D Co., Ltd., 523871 Dongguan, Guangdong, China
2. School of Traditional Chinese Medicine, Guangdong Pharmaceutical University, 510006 Guangzhou, Guangdong, China
3. Qilin Middle School, Nanshan Experimental Education Group, Nanshan District, 515100 Shenzhen, Guangdong, China

# The authors contributed equally to this work.

DOI: https://doi.org/10.62767/jecacm504.6382

Keywords

α-glucosidase
Inhibitory activity
Grey correlation
Partial least squares regression analysis
Molecular docking

* **Correspondence**

Dan Tang
School of Traditional Chinese Medicine, Guangdong Pharmaceutical University, 510006 Guangzhou, Guangdong, China
E-mail: tdpharm@126.com

Zhengming Qian
Dongguan HEC Cordyceps R&D Co., Ltd., 523871 Dongguan, Guangdong, China
E-mail: qianzhengming1982@126.com

Received: 14 October 2024
Revised: 29 November 2024
Accepted: 11 December 2024
Published: 13 December 2024

***Journal of Experimental and Clinical Application of Chinese Medicine* 2024; 5(4): 69-81.**

Abstract

Bistortae Rhizoma is a traditional Chinese medicine, which is the dried rhizome of *Polygonum bistorta* (PB). It has anti-inflammatory, antibacterial, antioxidant, anti-diabetic effects and so on. Among them, there exists a limited number of studies investigating the anti-diabetic effect of PB, and the specific ingredients responsible for this effect remain unclear. To rapidly screen α-glucosidase inhibitors in extracts of PB, this study explored the relation between effective components and enzyme inhibitory activity based on component-effect analysis, revealing its key active component. After the suppressing effect of extracts of PB from different batches on α-glucosidase was tested, high performance liquid chromatography (HPLC) was employed to plot fingerprint of PB and evaluate the similarity of fingerprint. Combined with HPLC-Q-Orbitrap high-resolution mass spectrometry (HRMS)/MS qualitative analysis, the grey relational analysis and partial least squares regression analysis were performed to screen active components, and molecular docking was used for activity validation. The results indicated that the 11 batches of PB extracts can effectively inhibit α-glucosidase, with half-maximal inhibitory concentration (IC_{50}) of 1.71-35.62 μg/mL, which had stronger inhibitory activity compared to the positive control acarbose (IC_{50} of 148.00 μg/mL). Among them, the PB07 batch of PB extract derived from Shandong province exerted the best inhibitory effect, with an IC_{50} of 1.71 μg/mL. The grey relational analysis and partial least squares regression analysis revealed that in the 11 batches of samples, 7 characteristic peaks had a relatively large correlation value with the inhibitory activity of PB on α-glucosidase, and the regression coefficient was positively correlated with inhibitory activity, indicating the importance of variables and high contribution. Through secondary mass spectrometry and database comparison, the 7 components were identified as 6-O-galloylglucose, L-tryptophan, (+)-gallocatechin-(4α→8)-(+)-catechin, deacetyl asperuloside, chlorogenic acid, catechin-5-O-glucoside, and digalloylglucose. It is noteworthy that the 7 components were all identified as α-glucosidase inhibitors in PB extract for the first time. Further molecular docking results showed that the binding energies of the 7 active components to α-glucosidase were all less than -6.0 kcal/mol, hinting significant inhibitory activity of α-glucosidase. Among them, the binding energy of catechin-5-O-glucoside was the lowest (-8.7 kcal/mol), which impacted enzyme active center mainly through hydrogen bonding. The results of this study provide research ideas for the development of hypoglycemic drugs using PB in the future.

1 Introduction

Diabetes, a metabolic disorder characterized by hyperglycemia, impacts 463 million adults worldwide currently, with number increasing at a rate of over 30 million people per year, according to the data released by the International Diabetes Federation [1]. Controlling blood glucose levels is critical to the prevention and treatment of diabetes. α-glucosidase inhibitor (AGI) inhibits the activity of α-glucosidase (AG), slows the release of glucose from starch and thereby reduces postprandial glucose [2]. At present, acarbose, voglibose, and miglitol are commonly used as AGI drugs in clinical practice, but long-term use can lead to significant gastrointestinal side effects [3]. Therefore, it is of great significance to seek natural AGIs that are highly effective and cost-efficient with minimal side effects from natural products.

Bistortae Rhizoma, the dried rhizome of *Polygonum bistorta* from the Polygonaceae family, is harvested in early spring when the plant begins to sprout or in the autumn when the stems and leaves are about to wither, which is cleaned of mud and sand, and sun-dried to remove fibrous roots [4]. The main therapeutic effects of Bistortae Rhizoma include clearing heat and detoxifying, reducing swelling, and stopping bleeding, which is primarily used to treat snake and insect bites, oral ulcers, abscess and scrofula, bloody dysentery and diarrhea, vomiting of blood or nosebleed and blood heat, and hemorrhoidal bleeding [5]. Modern pharmacological studies have shown that Bistortae Rhizoma has anti-inflammatory, antibacterial [6], antioxidant [7], antitumor [8], and cardiovascular-protective effects [9]. In recent years, there are reports discussing its anti-diabetic effects [10,11], but the active components responsible for its hypoglycemic activity remain unclear.

Spectrum-effect relationships have increasingly become a popular method in the research fields of traditional Chinese medicine (TCM) quality control and the pharmacodynamic substances of TCM [12,13]. The core of TCM spectrum-effect relationships lies in establishing a mapping relation between the TCM fingerprint and their pharmacological effects. Initially, the interrelationship between fingerprint and pharmacological effects is established, with correlation predictive methods including artificial neural networks, grey relational analysis (GRA), and correlation analysis; subsequently, the simple regression analysis is conducted for linear or nonlinear fitting to preliminarily determine the proportional contributions of multiple independent variables to a single dependent variable. Multiple linear regression and partial least squares regression (PLSR) analyses are utilized to elucidate the contribution rates of various chemical components to the pharmacological effects; finally, dimensionality reduction analysis of the data is performed to more comprehensively assess the contribution of each component to the overall pharmacological effect [14]. GRA can measure the relative degree of influence of one factor on others within a grey system, while PLSR analysis, based on multivariate statistical analysis, can also establish a regression model between two variables for predictive analysis of their relationship [15].

Therefore, this study explored the inhibitory effect of Bistortae Rhizoma on AG and the components responsible for its hypoglycemic action using GRA and PLSR method. Additionally, the molecular docking was utilized to clarify the interactions between active components and AG, providing a reference for the development of hypoglycemic drugs and laying the foundation for further development and utilization of Bistortae Rhizoma.

2 Experiment instruments, reagents and medicinal materials

2.1 Experiment instruments

Agilent 1260 high performance liquid chromatography (HPLC) (containing diode array detector, quaternary

low-pressure pump, and autosampler) (Agilent, USA); liquid chromatography-mass spectrometry (LC-MS)/MS (ThermoFisher, USA); P300H ultrasound equipment (ELMA, Germany); XPE205 scale (1/100000) (Mettler Toledo, USA); milli-Q ultrapure water purification system (Merck Millipore, Germany); sorvall ST40R centrifuge (ThermoFisher, USA); synergy H1 multimode microplate reader (Biotek, USA); similarity evaluation system for chromatographic fingerprint of TCM (Chinese Pharmacopoeia Commission, Version 2012).

2.2 Experiment reagents

AG lyophilized powder (#SLCC4854; Sigma-Aldrich, Shanghai, China); acarbose (95.00% purity, S25M11X109783, Shanghai Yuanye Biotechnology Co., LTD); 4-nitrophenyl- α -D-glucopyranoside (PNPG; K17A10B82914, Shanghai Yuanye Biotechnology Co., LTD); anhydrous sodium carbonate (AR level; 2021123101, Chengdu Kelong Chemical Co., LTD); absolute ethyl alcohol (AR level; 2023071901, Chengdu Kelong Chemical Co., LTD); acetonitrile (HPLC level; F4371440, Shanghai Anpu Experimental Technology Co., LTD); and acetic acid (HPLC level; E2124079, Aladdin, Shanghai, China).

2.3 Experiment medicinal materials

The origin information of the reference medicinal materials (PB01) and 10 batches of Bistortae Rhizoma samples (PB02-PB11) are as follows: PB01 from the reference medicinal materials of National Institutes for Food and Drug Control (121569-202203), PB02-PB07 from Shandong, and PB08-PB11 from Liaoning. All samples were identified as dried rhizomes of *Polygonum bistorta* (PB) by polymerase chain reaction (PCR) analysis.

3 Experiment methods

3.1 Chromatographic condition of fingerprint

The LC and MS conditions of Bistortae Rhizoma fingerprint previously published by our research group [16] were applied for analysis and detection.

LC conditions: Waters CORTECS T3 chromatographic column (4.6 mm × 100 mm, 2.7 μm); mobile phase of 0.1% acetic acid (A)-acetonitrile (B), gradient elution (0-2 min, 0-1% B; 2-5 min, 1%-2% B; 5-6 min, 2%-3% B; 6-8 min, 3%-6% B; 8-12 min, 6%-8% B; 12-20 min, 8%-10% B; 20-26 min, 10%-12% B; 26-28 min, 12% B; 28-37 min, 12%-13% B; 37-45 min, 13%-15% B; 45-50 min, 15% B; 50-60 min, 15%-18% B); test wavelength of 270 nm; column temperature of 25 ℃; flow velocity of 1 mL/min; and sample size of 5 μL.

MS conditions: MS analysis adopted positive and negative ion Full MS/dd-MS^2 mode scanning, with Full MS resolution of 70,000 and dd-MS^2 resolution of 17,500. Normalized collision energy of 10/20/40 eV; HESI ion source sheath as ion sources; airflow rate of 18 L/min; auxiliary gas flow rate of 6 L/min; scanning gas flow rate of 0.9 L/min; positive and negative mode spray voltage of 3.5 kV; capillary temperature of 400 ℃; auxiliary gas temperature of 450 ℃; scanning range of 100-1500 m/z.

3.2 Sample solution preparation for test

The control medicinal materials and 10 batches of Bistortae Rhizoma sample powder (filtered through No.3 filter; 0.5 g) were precisely weighed and obtained. Then, these samples were added with 15 mL 50% methanol solution, weighed, mixed, sonicated (20 min, 380 W, 37 kHz), cooled, compensated with weight, and centrifuged for 10 min (10,000 rpm/min). The supernatant was filtered via 0.22 μm millipore filter.

3.3 Control sample solution preparation

100 mg acarbose was precisely weighed and placed into 10 mL volumetric flask, and was dissolved by phosphate buffer solution (PBS) to 10 mL, yielding 10 mg/mL acarbose solution. The solution was stored at

4 ℃ and diluted to appropriate concentration when in use.

3.4 The inhibitory effect of Bistortae Rhizoma extracts on AG activity

The experiment about the inhibitory effect of Bistortae Rhizoma on AG activity followed the method described in the literature [17], with PNPG as the substrate and acarbose as the positive control. Blank group, control group, sample blank group, and sample group were constructed, with 3 parallels in each group. Reactants were added in sequence to the 96-well plate according to the dosage in Table 1. After the reaction, the 96-well plate was placed in a microplate reader and shaken for 5 min. The absorbance value (A value) at a wavelength of 405 nm was measured. The total volume of the reaction system was 200 μL. The inhibition rate I of Bistortae Rhizoma extracts on AG was calculated according to formula (1):

$$I(\%) = \left(1 - \frac{A_{sample} - A_{sample\ blank}}{A_{control} - A_{blank}}\right) \times 100\% \quad (1)$$

A_{sample}: Absorbance value of reaction solution in sample group; $A_{sample\ blank}$: Absorbance value of reaction solution in sample blank group; $A_{control}$: Absorbance value of reaction solution in control group; A_{blank}: Absorbance value of reaction solution in blank group.

The inhibitor concentration and its corresponding inhibition rate were input into the GraphPad Prism 8 software to draw the inhibition rate curve, and the half-maximal inhibitory concentration (IC_{50}) was calculated (Figure S1).

Table 1 Dosage and order of each reactant added (unit: μL).

Name of reagents	Group			
	Control group	Blank group	Sample group	Sample blank group
0.10 mol/L PBS (PH 6.8)	40	80	0	40
Sample solution	0	0	40	40
0.15 U/mL α-glucosidase solution	40	0	40	0
Fully mix, and incubate for 10 min at 37 ℃				
0.5 mg/mL PNPG solution	80	80	80	80
Fully mix, and incubate for 30 min at 37 ℃				
Add 40 μL of 1 mol/L sodium carbonate solution to terminate reaction				

3.5 Spectrum-effect relationship analysis

The GRA and PLSR analysis were performed to screen AG inhibitor of Bistortae Rhizoma extracts.

According to the calculation method in a study [18], the IC_{50} of 11 batches of Bistortae Rhizoma medicinal materials for AG acted as the parent sequence, and the characteristic peak area of 11 batches of Bistortae Rhizoma as the child sequence. The transformation of IC_{50} and characteristic peak area data were performed using the initial value transformation method to obtain the correlation results of antioxidant activity experiments. With the SPSSPRO online analysis platform (https://www.spsspro.com), the grey correlation degree can be directly obtained, simplifying the process of experimental data [19].

The area of each chromatographic peak representing the compound in the characteristic chromatogram served as the independent variable (X) and the inhibition rate of Bistortae Rhizoma on AG as the dependent variable (Y) [18,19], which were imported into SIMCA 14.0 software. The PLSR analysis was used for regression analysis.

3.6 Molecular docking

Ligand compound structures were downloaded from the PubChem database (https://pubchem.ncbi.nlm.nih.gov/) and Chem3D software was employed for energy minimization [20]. AG (PDB ID: 5NN8) was retrieved in the Protein Data Bank (PDB) database (https://www.rcsb.org/) and saved in pdb format. Pymol 2.5.0 was utilized to remove water molecules and modified ligands from the protein structure [21], and AutoDock Tools 1.5.6 was applied to perform hydrogenation and charge calculation on key targets [22], and convert the active components and AG into pdbqt format, followed by molecular docking using AutoDock Vina 1.1.2. Through the Protein-Ligand Interaction Profiler (PLIP) tool (https://projects.biotec.tu-dresden.de/plip-web/plip/index), the interactions between ligands and proteins were analyzed.

3.7 Data processing

GraphPad Prism 8 software was used for data statistics, inhibition rate curves were drawn, and IC_{50} values of extracts against AG were calculated.

4 Results

4.1 HPLC characteristic chromatogram of Bistortae Rhizoma

The analyses in line with the chromatographic conditions in section 3.1 revealed the chromatogram of 11 batches of Bistortae Rhizoma. The chromatograms were automatically integrated in the Agilent software system and exported in AIA format for storage. Then, they were imported into the "Similarity evaluation system for chromatographic fingerprint of TCM (Version 2012)" for analysis. With the chromatogram of sample PB11 as the reference spectrum, the median method was used for full peak automatic matching to generate HPLC fingerprint of 11 batches of Bistortae Rhizoma samples (PB01-PB11) (Figure 1). The similarity result range was 0.771-0.972. It is well known that PB is a perennial species with multiple producing areas, which can result in variability in the ingredient of samples collected at different harvesting times and locations. Furthermore, research indicates that variations in the color of PB pieces may also contribute to differences in the ingredient content of samples [23,24]. Consequently, although the chemical compositions of PB in different batches are similar, there still has differences in the ingredient contents.

Based on the retention time of each peak in the characteristic chromatogram of each sample, the peak areas of 29 characteristic peaks were identified, providing spectral data for subsequent spectrum-effect relationship analysis.

4.2 The *in vitro* inhibitory effect of Bistortae Rhizom on AG

In the experiment, the inhibitory effects of different batches of Bistortae Rhizoma extract on AG were compared and acarbose served as a positive control, with results expressed as IC_{50} values (μg/mL). The results showed the inhibitory capacities of the various batches of Bistortae Rhizoma against AG, in descending order of strength, as follows: PB07 (1.71) > PB02 (2.82) > PB08 (2.91) > PB05 (3.06) > PB03 (3.23) > PB04 (3.61) > PB11 (4.28) > PB09 (6.88) > PB06 (7.74) > PB10 (9.93) > PB01 (35.62) > acarbose (148.00). This indicated that all batches of the sample exerted a certain degree of inhibitory effect on AG activity, which were all stronger than the positive control acarbose, and demonstrated a dose-dependent inhibitory effect. Notably, the batch PB07 (from Shandong province) displayed the strongest inhibitory effect, being 86 times more potent than the positive control. Also, there were significant differences in the inhibitory effects of different batches of Bistortae Rhizoma on AG. For instance, the inhibitory effect of PB10 (from Liaoning province) was 3.5 times that of PB01 (the control medicinal material from the National Institutes for

Food and Drug Control). The considerable variation in inhibitory effects among batches may be attributed to the complexity of the extract components, where multiple compounds compete for the active site of AG, potentially leading to synergistic interactions that enhance the inhibitory effect [25].

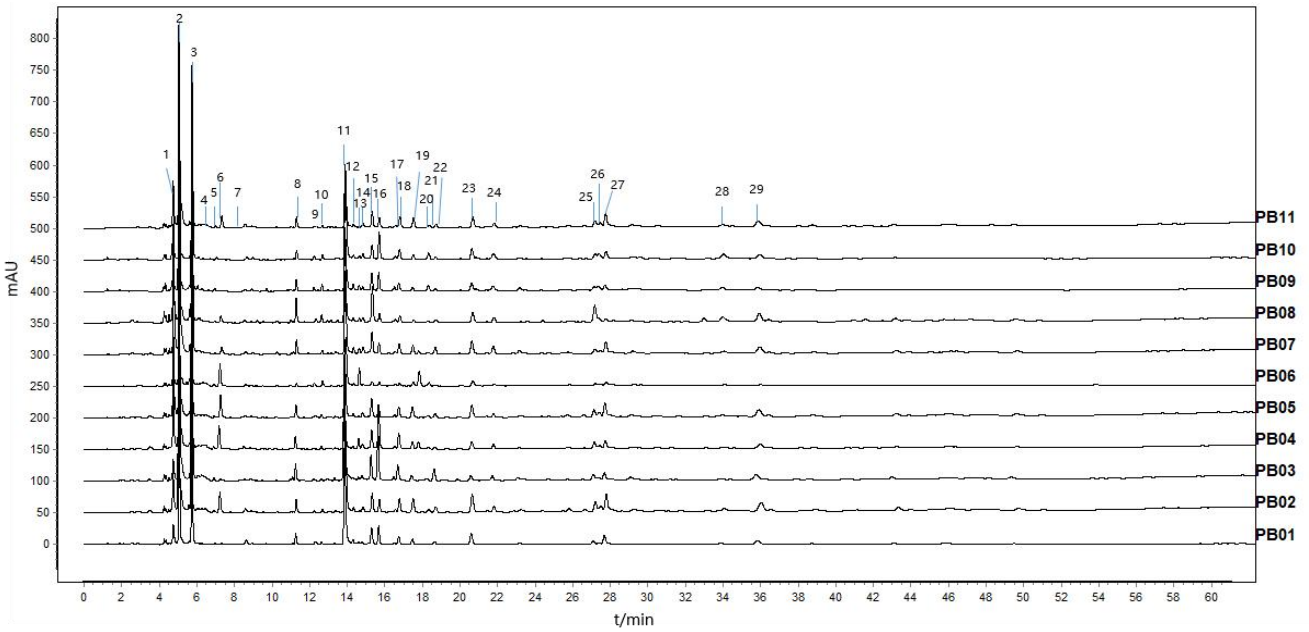

Figure 1 HPLC fingerprint of 11 batches of Bistortae Rhizoma samples.

4.3 Spectrum-effect relationship analysis

The current research confirmed that relative to other analysis methods, the relationship between spectrum and effect of TCM possesses the advantages of being efficient, economical, and environmentally friendly, and it can reflect the holistic concept of TCM [26,27]. In "spectrum-effect" analysis, the "spectrum" data typically refer to the quantitative data of chemical components in chemical chromatogram, while the "effect" data usually pertain to the pharmacological activity data of various extracts.

In this study, the "spectrum" data consisted of the peak areas of 29 major characteristic peaks in the fingerprint, and the "effect" data included the IC_{50} values of 11 batches of samples on AG. Subsequently, active components in Bistortae Rhizoma samples with inhibitory effects on AG were screened via GRA and PLSR.

4.3.1 GRA

After nondimensionalization of the peak areas of the characteristic chromatographic peaks in the fingerprint, the correlation coefficient was calculated to determine the degree of correlation, with a value closer to 1 indicating a better correlation. The correlation between the 29 characteristic peaks of Bistortae Rhizoma samples and their inhibitory capacity against AG was examined using the coefficient and ranking of grey relational degree. As shown in Table 2, the grey relational degrees of the 29 characteristic peaks were all ≥ 0.6, hinting that each peak had a certain inhibitory effect on AG. Among them, 8 characteristic peaks, No. 10, 11, 9, 7, 5, 16, 12, and 3 (in descending order), had a relational degree ≥ 0.8, suggesting that these 8 compounds were the main contributors to the inhibitory effect of Bistortae Rhizoma on AG.

4.3.2 PLSR analysis

Utilizing SIMCA 14.1 software, the IC_{50} values of AG of 50% methanol extract from 11 batches of Bistortae Rhizoma as the dependent variable and the areas of characteristic peaks as the independent variables, PLSR analyses were employed to calculate the

standardized regression coefficients and Variable Importance in Projection (VIP) values, assessing the association between Bistortae Rhizoma and its inhibitory effect on AG. The results indicated that, based on the IC_{50} value as an indicator, peaks that were positively correlated with the IC_{50} values included No. 7, 9, 11, 3, 23, 16, 12, 2, 27, 20, 13, 10, 15, 8, 21, and 18 (in descending order), while peaks that were negatively correlated with the IC_{50} values were No. 29, 24, 6, 17, 1, 14, 25, 22, 4, 28, 19, 26, and 5 (Figure 2). In the PLSR analysis of the IC_{50} values, characteristic peaks with VIP values > 1 included No. 7, 11, 3, 9, 23, 2, 12, 27, 15, 8, 10, 18, 16, and 5 (Figure 3), suggesting that compounds represented by these peaks were significantly correlated with the strength of Bistortae Rhizoma's inhibitory effect on AG.

Table 2 Correlation between the peak areas of characteristic peaks in the fingerprint of Bistortae Rhizoma and the IC_{50}.

Correlation results			Correlation results		
Evaluation item (No. of peak)	**Degree of correlation**	**Rank**	**Evaluation item (No. of peak)**	**Degree of correlation**	**Rank**
10	0.823	1	15	0.774	16
11	0.822	2	18	0.772	17
9	0.820	3	14	0.772	18
7	0.820	4	8	0.771	19
5	0.818	5	1	0.768	20
16	0.817	6	19	0.764	21
12	0.811	7	13	0.761	22
3	0.802	8	4	0.761	23
23	0.797	9	22	0.760	24
21	0.792	10	25	0.757	25
2	0.790	11	6	0.715	26
17	0.784	12	28	0.710	27
24	0.784	13	29	0.701	28
26	0.781	14	20	0.697	29
27	0.774	15			

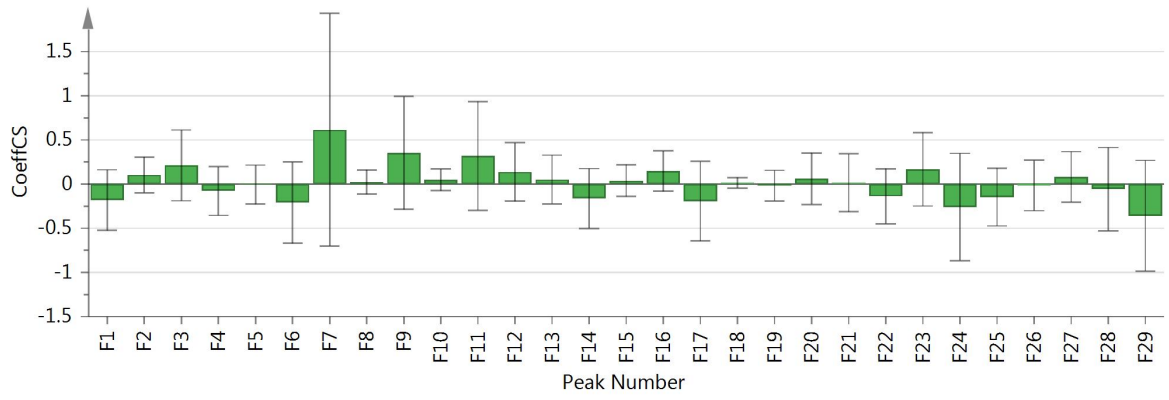

Figure 2 Partial regression coefficient between characteristic peak of HPLC fingerprint of Bistortae Rhizoma and enzyme inhibition index.

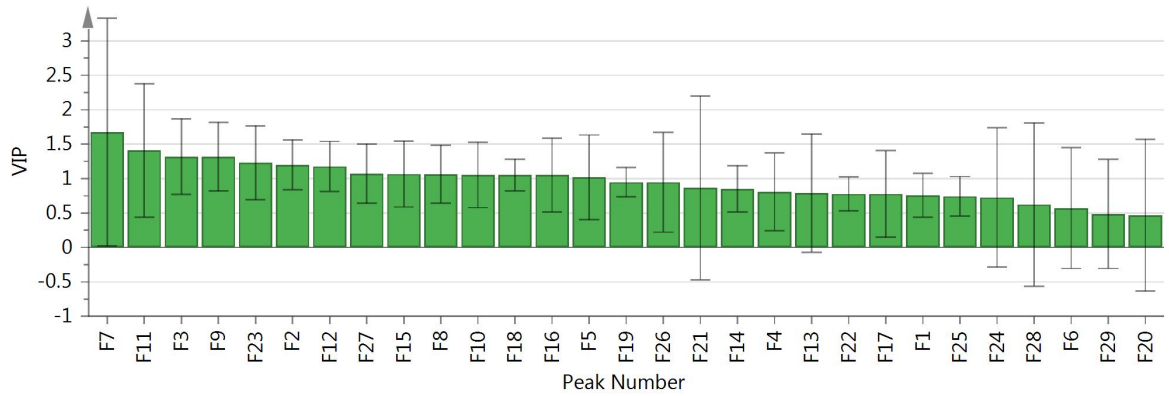

Figure 3 VIP value between characteristic peak of HPLC fingerprint of Bistortae Rhizoma and enzyme inhibition index.

According to the two indicators of comprehensive regression coefficients > 0 and VIP > 1, characteristic peaks of No. 7, 11, 3, 9, 23, 2, 12, 27, 15, 8, 10, 18, and 16 were ultimately identified as active components influencing the inhibitory effect of Bistortae Rhizoma on AG in the PLSR model.

Considering the results from both GRA and the PLSR model, common results were taken to draw more reliable conclusions. A total of 7 principal components were predicted to affect the inhibitory effect of different batches of Bistortae Rhizoma on AG, corresponding to peaks 3, 7, 9, 10, 11, 12, and 16.

4.4 HPLC-MS component identification

Through MS analysis as described in Section 3.1, the secondary MS fragment information of the aforementioned 7 major active chromatographic peaks was obtained and summarized in Table 3. By integrating data from Massbank database, PubChem database, and data of relevant literature, the chromatographic peaks 3, 7, 9, 10, 11, 12, and 16 were identified as 6-O-galloylglucose, L-tryptophan, (+)-gallocatechin-(4 α → 8)-(+)-catechin, deacetyl asperuloside, chlorogenic acid, catechin-5-O-glucoside, and digalloylglucose, respectively. The 7 compounds consisted of 3 phenolic acids (peaks 3, 11, 16), 2 flavonoids (peaks 9, 12), 1 iridoid (peak 10), and 1 amino acid (peak 7). The seven components were all identified as AGIs in Bistortae Rhizoma for the first time. The findings will contribute to enhancing the quality assessment standards of Bistortae Rhizoma, thereby facilitating its potential for extensive development opportunities.

4.5 Molecular docking verification

Molecular docking is a computational simulation method that studies the interactions between ligands and receptors, which can be used to predict the binding modes and affinities between ligands and receptors. In recent years, molecular docking has been widely applied to investigate the biological activities of natural enzyme inhibitors [28-30]. To verify the activity of 7 potential enzyme inhibitors in Bistortae Rhizoma, molecular docking analysis was conducted between these components and AG (Table 4). The results unraveled that the binding energies (kcal/mol) of the 7 potential enzyme inhibitors with AG were as follows: catechin-5-O-glucoside (-8.7) > digalloylglucose (-7.5) > chlorogenic acid (-7.3) > (+)-gallocatechin-(4 α → 8)-(+)-catechin (-7.2) > 6-O-galloylglucose (-6.6) > L-tryptophan and deacetyl asperuloside (-6.4), all of which were less than -6.0 kcal/mol, suggesting that the 7 potential enzyme inhibitors had significant inhibitory effects on AG.

Further research found that the 7 potential enzyme inhibitors primarily docked with the active center of enzymes through hydrogen bonding, hydrophobic interactions, and salt bridge interactions (Figure 4).

For instance, 6-O-galloylglucose formed six hydrogen bonds with the amino acid residues ASP282, ALA284, ASP404, ARG600, and ASP616 of AG, and interacted with the TRP376, TRP481, and PHE649 amino acid residues of AG through hydrophobic interactions (Figure 4a). Deacetyl asperuloside forms five hydrogen bonds with the amino acid residues ARG608, HIS717, GLU866, VAL867, and LEU868 of AG, which hydrophobically interacted with the amino acid residues MET363, ARG594, and LEU865 of AG, and also interacted with the amino acid residues HIS584, ARG594, and HIS717 of AG through salt bridge interactions (Figure 4c). Similarly, digalloylglucose docked with the active center of enzymes through hydrogen bonding (Figure 4g). (+)-gallocatechin-(4α→8)-(+)-catechin and chlorogenic acid docked with the active center of enzymes through hydrogen bonding and hydrophobic interactions (Figure 4d and 4e). L-tryptophan and catechin-5-O-glucoside docked with the active center of enzymes through hydrogen bonding, hydrophobic interactions, and salt bridge interactions (Figure 4b and 4f).

Collectively, based on the spectrum-effect relationship, 7 potential AG enzyme inhibitors were identified, and their activities were validated through molecular docking. Among them, catechin-5-O-glucoside had the lowest binding free energy (-8.7 kcal/mol) and primarily interacted with the active center of enzymes through hydrogen bonding, demonstrating strong inhibitory activity against AG enzyme.

Table 3 HPLC-MS identification data of chemical components of Bistortae Rhizoma.

No.	Retention time (min)	Compound	Formula	Ion pattern	Molecular ion (m/z)	Ppm	Fragment ion (m/z)	Type	Ref.
3	7.91	6-O-galloylglucose	$C_{13}H_{16}O_{10}$	$[M-H]^-$	331.0673	2.35	271.0460, 211.0247, 169.0135, 125.0234	Phenolic acids	[31]
7	9.79	L-tryptophan	$C_{11}H_{12}O_2N_2$	$[M-H]^-$	203.0820	1.22	142.0659, 116.0501, 74.0242	Amino acid	[32]
9	13.03	(+)-gallocatechin-(4α→8)-(+)-catechin	$C_{30}H_{26}O_{13}$	$[M-H]^-$	593.1313	3.01	467.0986, 407.0776, 289.0721, 125.0233	Flavonoids	[33]
10	13.30	deacetyl asperuloside	$C_{16}H_{20}O_{11}$	$[M-H]^-$	387.0936	3.6	267.0725, 249.0618, 211.0608, 137.0239	Iridoids	[34]
11	14.58	chlorogenic acid	$C_{16}H_{18}O_9$	$[M-H]^-$	353.0885	2.67	191.0556, 179.0337, 161.0238	Phenolic acids	[31]
12	15.09	catechin-5-O-glucoside	$C_{21}H_{24}O_{11}$	$[M-H]^-$	451.1249	1.91	289.0723, 245.0819, 203.0710, 109.0283	Flavonoids	[31]
16	16.23	digalloylglucose	$C_{20}H_{20}O_{14}$	$[M-H]^-$	483.0787	2.52	271.0463, 211.0245, 193.0137, 169.0134	Phenolic acids	[31]

Table 4 Molecular docking results between Bistortae Rhizoma and AG.

Ligand	Residual base	Interaction relationship	Affinity (kcal/mol)
6-O-galloylglucose	8	ASP282, ALA284, ASP404, ARG600, ASP616, TRP376, TRP481, PHE649	-6.6
L-tryptophan	8	MET363, HIS584, GLU866, LEU865, LEU868, VAL867, ARG594, HIS717	-6.4
deacetyl asperuloside	9	ARG608, HIS717, GLU866, VAL867, LEU868, MET363, ARG594, LEU865, HIS584	-6.4
(+)-gallocatechin-(4α→8)-(+)-catechin	7	MET363, HIS584, ARG608, HIS717, GLU866, GLU869, LEU865	-7.2
chlorogenic acid	6	GLU196, PHE490, ARG608, TYR609, LEU577, ILE581	-7.3
catechin-5-O-glucoside	9	TYR360, MET363, ARG594, ARG608, HIS717, VAL867, LEU868, PHE362, HIS584	-8.7
digalloylglucose	8	ASP91, PRO94, LYS96, ILE98, TRP126, CYS127, ARG275, ARG331	-7.5

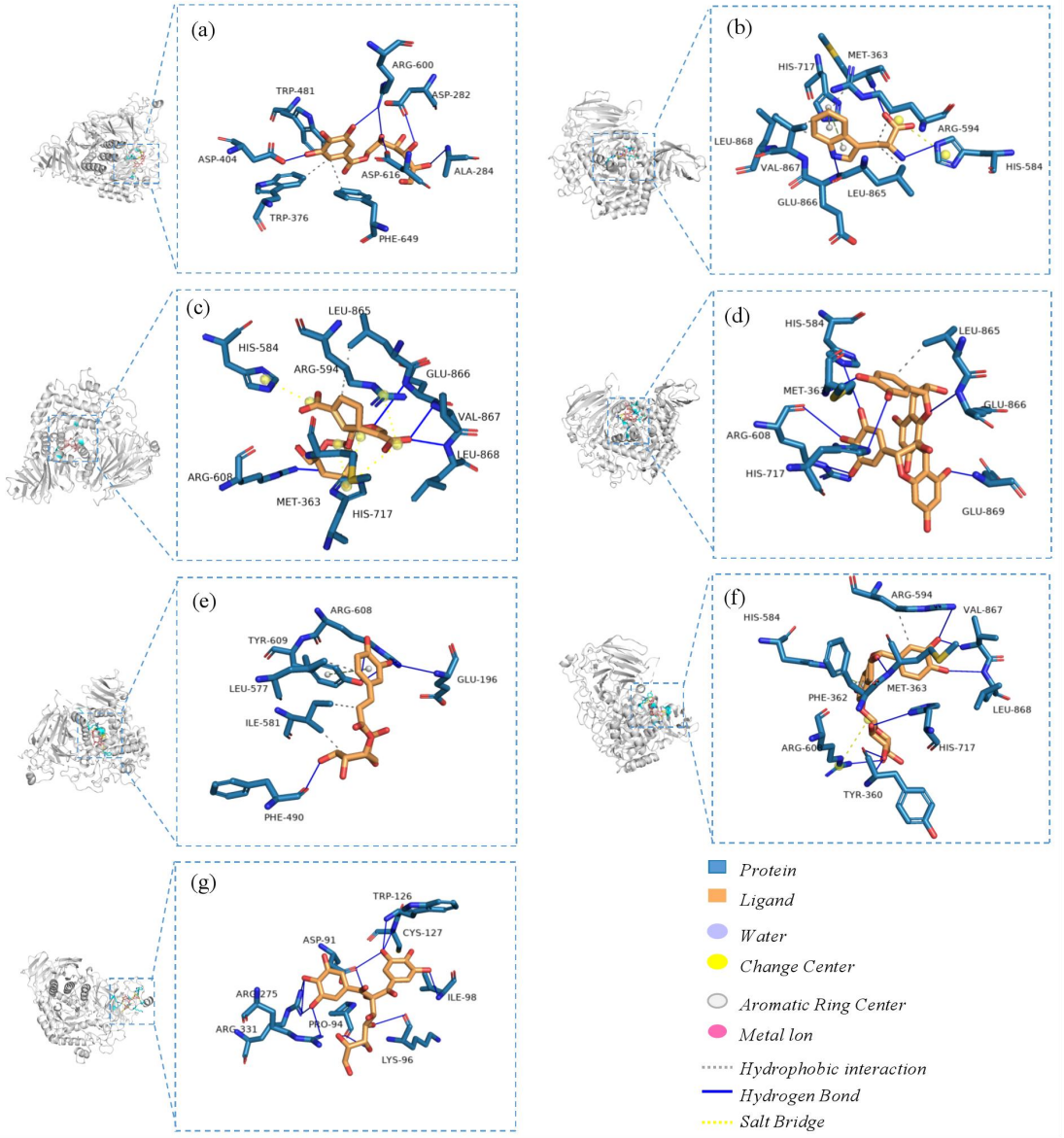

Figure 4 Molecular docking model of 7 compounds with AG. 6-O-galloylglucose (a); L-tryptophan (b); deacetyl asperuloside (c); (+)-gallocatechin-(4α→8)-(+)-catechin (d); chlorogenic acid (e); catechin-5-O-glucoside (f); digalloylglucose (g).

5 Conclusion

Combining fingerprint spectrum analysis, HPLC-Q-Orbitrap HRMS/MS analysis, and enzyme inhibitory activity analysis, this study employs GRA and PLSR to screen 7 potential enzyme inhibitors from Bistortae Rhizoma, including 6-O-galloylglucose, L-tryptophan, deacetyl asperuloside, (+)-gallocatechin-(4α→8)-(+)-catechin, chlorogenic acid, catechin-5-O-glucoside, and digalloylglucose, which are all proved to be AGIs in Bistortae Rhizoma extract for the first time. The activity of these inhibitors is validated through molecular docking, elucidating the interactions between these active components and the enzyme. These findings reveal the specific bioactive components of Bistortae Rhizoma in anti-diabetic activity, which contributes to the development of Bistortae Rhizoma products with anti-diabetic activity and provides a scientific basis for improving the quality evaluation of Bistortae Rhizoma and its related products.

Acknowledgements

Not applicable.

Conflicts of Interest

The authors declare that they do not have any commercial or associative interest that represents a conflict of interest in connection with the work.

Author Contributions

Conceptualization, Z.Q. and D.T.; Funding acquisition, Z.Q.; Investigation, Q.H., W.Y., and L.X.; Methodology, Q.H., W.Y., and X.L.; Validation, Q.H., W.Y., and X.L.; Data curation, Q.H., W.Y., X.L., and L.X.; Project administration, Z.Q. and D.T.; Supervision, Z.Q. and D.T.; Writing—original draft, Q.H., W.Y., and Z.Q.; Writing—review and editing, Q.H., W.Y., X.L., L.X., D.T., and Z.Q.; Resources, Z.Q. All authors have read and agreed to the published version of the manuscript.

Ethics Approval and Consent to Participate

The manuscript didn't involve any human or animal subjects, therefore no ethical approval was required for this article.

Funding

This study was financially supported by the Key-Area Research and Development Program of Guangdong Province (2020B1111110007).

Availability of Data and Materials

The data presented in this study are available on request from the corresponding author.

Supplementary Materials

The following supporting information can be downloaded at: https://ojs.exploverpub.com/index.php/jecacm/article/view/167/sup. Figure S1: The IC_{50} curves of AG and PB samples.

References

[1] Yagasaki K, Muller CJF. The Effect of Phytochemicals and Food Bioactive Compounds on Diabetes. *International Journal of Molecular Sciences* 2022; 23(14): 7765.

[2] Lansakara LHMPR, Liyanage R, Perera KA, et al. Nutritional Composition and Health Related Functional Properties of *Eleusine coracana* (Finger Millet). *Procedia Food Science* 2016; 6: 344-347.

[3] Mushtaq A, Azam U, Mehreen S, et al. Synthetic α-Glucosidase Inhibitors as Promising Anti-Diabetic Agents: Recent Developments and Future Challenges. *European Journal of Medicinal Chemistry* 2023; 249: 115119.

[4] Chinese Pharmacopoeia Commission. *Pharmacopoeia of the People's Republic of China*, 1st ed.; China Medical Science Press: Beijing, China, 2020; p. 301.

[5] Wang DQ, Yin T, Han ZB, et al. Study on the Different Regions of Resource Investigate and Evaluation of *Polygonum bistorta* L. Quality. *Modernization of Traditional Chinese Medicine and Materia Medica-World Science and Technology* 2019; 21(12): 2764-2769.

[6] Cui J, Zhao KJ. Antibacterial Effect Evaluation of Bistortae Rhizoma Against *Escherichia coli* by Microcalorimetry. *Chinese Journal of Experimental Traditional*

Medical Formulae 2018; 24(12): 57-61.

[7] Li S, Tang L, Chan D, et al. Seperation and purification of *Polygonum bistorta* and the screening of the active antioxidant fraction. *West China Journal of Pharmaceutical Sciences* 2016; 31(2): 121-123.

[8] Liu YH, Weng YP, Lin HY, et al. Aqueous Extract of Polygonum Bistorta Modulates Proteostasis by Ros-Induced Er Stress in Human Hepatoma Cells. *Scientific Reports* 2017; 7(1): 41437.

[9] Wang HN, Huang BS, Zhan ZL, et al. Latest Research Progress of Chemical Constituents and Pharmacological Activities of *Polygonum bistorta* L. *Modernization of Traditional Chinese Medicine and Materia Materia-World Science and Technology* 2020; 22(8): 2998-3007.

[10] Bauer I, Rimbach G, Nevermann S, et al. In-Vitro Antidiabetic Activity of a Bistorta Officinalis Delarbre Root Extract Can Not be Confirmed in the in-Vivo Models Hen's Egg Test and Drosophila Melanogaster. *Journal of Physiology and Pharmacology* 2023; 74(1): 37245231.

[11] Sharafetdinov KK, Kiseleva TL, Kochetkova AA, et al. Promising Plant Sources of Anti-Diabetic Micronutrients. *Journal of Diabetes & Metabolism* 2017; 8(12): 1-7.

[12] Malherbe CJ, Beer D, Joubert E. Development of On-Line High Performance Liquid Chromatography (HPLC)-Biochemical Detection Methods as Tools in the Identification of Bioactives. *International Journal of Molecular Sciences* 2012; 13(3): 3101-3133.

[13] Wang F, Cao J, Li Y, et al. Study of Quality Markers of Antiuric Acid Formula by Grey Relational Analysis. *SN Applied Sciences* 2021; 3(6): 661.

[14] Pan J, Liu DS, Yan GM. Research progress in the application of data analysis to the spectral effect relationship of traditional Chinese medicine. *Acta Chinese Medicine and Pharmacology* 2018; 46(4): 119-122.

[15] Xiao RY, Teng PP, Hu C, et al. Research Progress in Application of Partial Least Squares Regression Analysis in the Spectrum-effect relationship of Traditional Chinese Medicine. *Liaoning Chemical Industry* 2020; 49(3): 303-305.

[16] Li XF, Yang WQ, Huang Q, et al. Study on the spectrum effect relationship between high performance liquid chromatography fingerprint and antioxidant activity of *Polygonum bistorta* L. *Journal of Guangdong Pharmaceutical University* 2024; 40(4): 9-17.

[17] Zheng X, Li GH, Wang X, et al. Screening and Strains Identification of α -Glucosidase Inhibitory Activity from Endophytes of *Tripterygium hypoglaucum*. *Chinese Journal of Experimental Traditional Medical Formulae* 2015; 21(23): 122-125.

[18] Liang H, Tao CL, Liu YM, et al. Study on the quality evaluation of Salvia chinensis based on multi-component quantitative analysis combined with chemometrics. *Journal of Guangdong Pharmaceutical University* 2023; 39(1): 51-60.

[19] Azzeh M, Neagu D, Cowling PI. Fuzzy grey relational analysis for software effort estimation. *Empirical Software Engineering* 2010; 15(1): 60-90.

[20] Kaur T, Madgulkar A, Bhalekar M, et al. Molecular docking in formulation and developmen. *Current Drug Discovery Technologies* 2019; 16(1): 30-39.

[21] Saikia S, Bordoloi M. Molecular docking: Challenges, advances and its use in drug discovery perspective. *Current Drug Targets* 2019; 20(5): 501-521.

[22] Chen HJ, Qin HY, Long F, et al. Screening of High-Affinity α-Glucosidase Inhibitors from Cichorium Glandulosum Boiss. et Hout Seed Based on Ultrafiltration Liquid Chromatography-Mass Spectrometry and Molecular Docking. *Chinese Journal of Analytical Chemistry* 2017; 45(6): 889-897.

[23] Dong JM, Cui J, Zhao XM, et al. Comparative study on HPLC-MS fingerprint of Bistortae Rhizoma prepared slides in 2 different colors. *Chinese Journal of Pharmaceytical Analysis* 2017; 37(8): 1503-1508.

[24] Guo CW, Xu WL, Xu R, et al. Research on Grade Classification of Quanshen (*Polygonum bistorta*) Based on "Quality Evaluation through Morphological Identification" and Comprehensive Evaluation Index. *Chinese Archives Of Traditional Chinese Medicine* 2024; 42(9): 240-245.

[25] Li YS. Study on α-Glucosidase Inhibitory Activity and Mechanism of Indirubin Derivative. Master's Degree. Tianjin University of Science and Technology: Tianjin, China, 2017.

[26] Li R, Yan ZY, Li WJ, et al. Study on the establishment of spectrum-effect relationship of traditional Chinese medicine. *Education of Chinese Medicine* 2002; 2: 62.

[27] Zhang Q, Yang YT. Overview of the Research Status of the Relationship between Spectrum and Effect of Traditional Chinese Medicine. *Lishizhen Medicine and Materia Medica Research* 2022; 33(3): 680-683.

[28] Saber FR, Ashour RM, EI-Halawany AM, et al. Phytochemical profile, enzyme inhibition activity and molecular docking analysis of *Feijoa sellowiana* O. Berg.

Journal of Enzyme Inhibition and Medicinal Chemistry 2021; 36: 618-626.

[29] Khurshid U, Ahmad S, Saleem H, et al. Multifaced assessment of antioxidant power, phytochemical metabolomics, in-vitro biological potential and in-silico studies of *Neurada procumbens* L.: An important medicinal plant. *Molecules* 2022; 27: 5849.

[30] Cai YZ, Wu LF, Lin X, et al. Phenolic profiles and screening of potential α -glucosidase inhibitors from *Polygonum aviculare* L. leaves using ultra-filtration combined with HPLC-ESI-qTOF-MS/MS and molecular docking analysis. *Industrial Crops and Products* 2020; 154: 112673.

[31] Pawłowska KA, Hałasa R, Dudek MK, et al. Antibacterial and Anti-Inflammatory Activity of Bistort (Bistorta Officinalis) Aqueous Extract and Its Major Components. Justification of The Usage of The Medicinal Plant Material as a Traditional Topical Agent. *Journal of Ethnopharmacology* 2020; 260: 113077.

[32] Cai WF, Wang Y, Jin WF, et al. Chemical constituents of Qiang medicine Primula chungensis by UPLC-Q-Exactive-Orbitrap-MS. *Natural Product Research and Development* 2023; 35(6): 986-996.

[33] Liu YC, Dai YP, Wang BL, et al. Rapid Analysis of Tannins from Pomegranate Peel Based on UPLC-Quadrupole/Exactive Orbitrap Mass Combined with Diagnostic Ions Filter. *Chinese Archives of Traditional Chinese Medicine* 2023; 41(5): 71-79.

[34] Shen Y, Zhang Q, Liu MQ, et al. Research on chemical components and biological activities of the iridoids in Morinda genus. *Journal of Pharmaceutical Practice and Service* 2020; 38(2): 110-114,119.